TECHNICAL TRANSACTIONS 3/2018
CZASOPISMO TECHNICZNE 3/2018
ENVIRONMENTAL ENGINEERING
DOI: 10.4467/2353737XCT.18.046.8341
SUBMISSION OF THE FINAL VERSION: 5/3/2018

Tomasz Siuta (tsiuta@iigw.pl)
Institute of Hydraulic Engineering and Water Management, Department of Hydraulics and Hydrology, Cracow University of Technology

The impact of deepening the stilling basin on the characteristics of hydraulic jump

Wpływ zagłębienia niecki wypadowej na zmiany charakterystyki odskoku hydraulicznego

Abstract

In this article, the results of computational fluid dynamic (CFD) modelling of the hydraulic jump conditions occurring in the experimental prismatic rectangular stilling basin with sudden crosswise expansion are presented. The FLOW 3D software program was used to numerically solve Reynolds Navier-Stokes (RANS) equations with the application of the k-ε turbulence model. The influence of the depth magnitude of the stilling basin and the ending sill installation on the hydraulic jump turbulent characteristics and submergence condition changes was investigated. Based on the results of the numerical modelling, it was found that various spatial flow processes contribute to the submergence condition of the hydraulic jump. These processes include: crosswise flow expansion within the stilling basin; local tail water surface level increase and total head loss due to vertical flow contraction; installation of the additional terminal sill. This contribution to the submergence condition allows a reduction in the required depth of the stilling basin, calculated on the basis of a one-dimensional simplified approach without consideration to the spatial characteristic of the hydraulic jump.

Keywords: the stilling basin, the hydraulic jump, CFD modelling, conjugated depth, energy dissipation

Streszczenie

W artykule przedstawiono przykład zastosowania techniki CFD (Numeryczna Mechanika Płynów) do modelowania warunków wystąpienia odskoku hydraulicznego w eksperymentalnej pryzmatycznej niecce wypadowej z nagłym poszerzeniem. W celu rozwiązania równań Reynolds Navier-Stokes (RANS) wraz z modelem turbulencji typu k-ε użyto programu FLOW 3D. Przedmiotem badania był wpływ głębokości niecki wypadowej i wysokości progu wylotowego na zmianę charakterystyki przepływu turbulentnego i warunki zatopienia odskoku. Na podstawie uzyskanych wyników modelowania stwierdzono, iż przestrzenne procesy przepływu, takie jak: poprzeczna ekspansja strumienia w niecce wypadowej, lokalne podniesienie poziomu zwierciadła wody dolnej na skutek kontrakcji pionowej przepływu w przekroju wyjściowym z niecki, instalacja progu wylotowego mogą przyczynić się w istotny sposób do zatopienia odskoku hydraulicznego, a tym samym pozwalają na redukcję wymaganej głębokości niecki wypadowej obliczanej na podstawie uproszczonej jednowymiarowej analizy przepływu bez uwzględnienia przestrzennego charakteru badanego odskoku hydraulicznego.

Słowa kluczowe:

1. Introduction

Hydraulic structures like dams, weirs and culverts release an elevated mass of water within upstream river reach – this leads to the formation of a hydraulic jump just downstream of the structure within the river channel. It is a very important challenge for engineers to investigate different techniques which allow to change the characteristics of hydraulic jump in that way which is preferable to keep the process of energy dissipation under control. One of these techniques is appropriate designing of the stilling basin. Studies of stilling basin performance are of great importance for the construction, maintenance and safety of hydraulic structures. Increases to the efficiency of energy dissipation reduce the risk of downstream erosion of the structure which could constitute a threat to its stability. Designing of stilling basin requires the calculation of its depth and length to satisfy hydraulic jump submergence condition for given design discharge and corresponded tail water level range. In addition to these specifications, structures such as baffle blocks, sills, corrugated beds may be implemented within the stilling basin to enhance the processes of energy dissipation. CFD numerical modelling of the complex spatial flow may be implemented as an important tool to improve the efficiency of the design and exploitation procedures of the stilling basin.

In the article, results of numerical modelling testing of the hydraulic jump within the stilling basin both with and without the sill are presented – this testing was performed with the application of the FLOW 3D software program [1].

The main objective of this numerical test was the investigation of the hydraulic jump stabilisation and submergence within the stilling basin with rectangular cross section (Fig. 1). Flow is discharged into the stilling basin via a chute of the width which is half the width of the stilling basin. This allows for flow expansion in a crosswise direction. Previous literature concerns the experimental [2, 3] and theoretical [4] investigation of the impact of sudden channel expansion on the hydraulic jump performance; however, there is a shortage of numerical modelling of such cases. The hydraulic jump submergence condition for different depths of stilling basin, both with and without the ending sill, was tested. Additionally, the shear stress distribution at the bottom of the stilling basin and the downstream channel reach was determined under condition of the design discharge.

The CFD method allows the simulation of flow processes by discretisation and numerical solution of Navier-Stokes equations for each computational cell [5]. Many researchers apply this method to investigate hydraulic jump performance within a stilling basin or river channel with different turbulent energy dissipation techniques and devices. The majority of works focus on experimental data fitting [6], testing different turbulent models like k-ε, the RNG, hybrid models [7] and air entrainment influence on hydraulic jump characteristics [8, 9]. Others works are focused on hydraulic jump design issues relating to hydraulic structures. There are some techniques inducing and controlling hydraulic jump through the use of application structures like macro-roughness, sudden drop, terminal sill and stilling basin. One of these technique is the application of corrugated beds [10] which increase Reynolds stresses and decrease the second conjugated depth of jump by causing strong turbulence in flow. Numerical simulation of hydraulic jump on a corrugated bed

was evaluated using standard *k*-ε turbulent model [11] and achieved strong agreement with experimental data.

In one study, a FLOW-3D model was applied to evaluate the potential of abrasion in the stilling basin of Colombia Power Plant and to aid the optimisation of the recommended modification of the structure. The model reproduced the recirculation due to the formation of the roller associated to hydraulic jump and small recirculation just downstream of the terminal sill [12].

The USBR (U.S. Bureau of Reclamation) type III stilling basin [13], for which design procedures are well established and based on experimental laboratory data, is commonly used in the US. It is generally applied on canal structures, small outlet works, and small spillways dedicated for cases of Froude numbers above four. Recently some literature has appeared concerning CFD numerical investigation of influence of adverse hydraulic conditions on the hydraulic jump characteristics. Researchers obtain a detailed insight of the role of each basin element and their adapting roles when insufficient tail water conditions exist [14]. Furthermore stepped spillway hydraulic flow condition influence on the size of the basin dimensions was explored. An interesting geometric modification of the USBR basin type is the application of convergence walls. The hydraulic jump performance change due to this geometrical modification which was tested by CFD model [15] and researchers find that in all the discharges cases, the hydraulic jump in the basin with converged walls has larger efficiency of kinetic energy dissipation in comparison to the case of the stilling basin with parallel walls.

2. Numerical experiment

2.1. Geometry of the hydraulic structure

The geometric domain of the model includes: discharging tank, chute-weir, stilling basin and short channel reach. The chute-weir invert is 4 m above the bottom of the channel (Fig. 1). The width of the chute is 5 m and the width of the stilling basin is 10 m. The length of the basin was assumed based on the second conjugated height (h_2) approximation (Table 1) and is 13 m. The magnitude of the design discharge is 50 m^3/s, the corresponding upstream water head is 6.6 m and tail water head is 2 m above the bottom of the channel (Fig. 1). The different depth magnitudes of the stilling basin were investigated to control the hydraulic jump submergence condition.

The following variants of the stilling basin were investigated:

*S*2 – the stilling basin of the depth d = 2 m without the sill and with ending wall inclination 1:1 (Fig. 1)
*S*1 – the stilling basin of the depth d = 1 m without the sill and with vertical ending wall
*S*05 – the stilling basin of the depth d = 0.5 m without the sill and with vertical ending wall
*S*05*p* – the stilling basin of the depth d = 0.5 m with the terminal sill (h_s = 0.5 m)
*S*02*p* – the stilling basin of the depth d = 0.2 m with the terminal sill (h_s = 0.5 m)

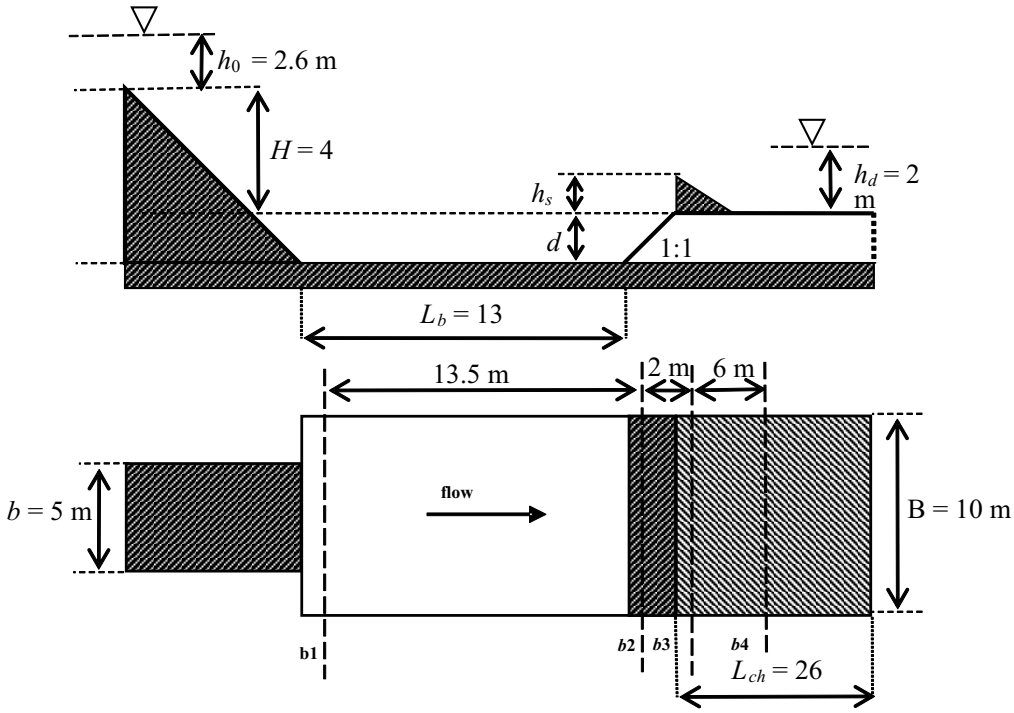

Fig. 1. The stilling basin geometry with the control cross sections ($b1$–$b4$)

2.2. The simplified hydraulic design of the stilling basin

Analysis of the M-y Diagram indicates that the larger value of the unitary flow discharge (q), the smaller the difference of the conjugated depths (h_2–h_1) and the smaller the amount of dissipated energy by the hydraulic jump [16]. The crosswise flow expansion results in a decrease of the unitary flow discharge value at the downstream cross section of the stilling basin – this contributes to more efficient energy dissipation ($\Delta H/H_1$) within the stilling basin (Table 1).

The theoretical depth (Table 1) of the stilling basin (which allow for the hydraulic jump submergence for given flow conditions) was calculated based on one-dimensional hydraulic analysis of the hydraulic jump within the prismatic rectangular channel [16] for the given design *see above note* discharge (50 m^3/s). Such simplified hydraulic analysis in the case of the crosswise flow expansion may lead to significant overestimation of the depth required for hydraulic jump submergence within the stilling basin; therefore, CFD numerical modelling was used to verify this condition.

In order to achieve a reference framework for the tested variants of the stilling basin with flow expansion, the hydraulic jump conjugated depths (eq. 1 and eq. 2), total head loss (ΔH) and corresponding depth of the theoretical stilling basin (required for submergence of the hydraulic jump) were calculated (Table 1) based on two cases of unitary flow rate magnitudes uniformly distributed in the cross section of the theoretical stilling basin without crosswise

flow expansion. The first flow rate magnitude q_1 = 10 m²/s is a value associated with the chute width (5 m) and second magnitude q_2 = 5 m²/s with the width of the tested stilling basin (10 m) for the given design discharge (Q = 50 m³/s) and tail water head (h_d = 2 m). The approximation of the first conjugated depth was calculated based on the Bernoullie equation (eq. 1) assuming the value of the velocity coefficient φ = 0.9. The sequent conjugated, depth was calculated based on the conservation of momentum flux applied for one-dimensional flow in a prismatic rectangular channel (eq. 2). Finally, the reference depth values (d) of the theoretical stilling basin required to satisfy submergence of the hydraulic jump under condition of the investigated unitary flow values (q_1 and q_2) were fixed (Table 1).

$$h_1 = \frac{Q}{\varphi \times b \times \sqrt{2g\left(H_{up} - h_1\right)}} \tag{1}$$

where:

h_1 – first conjugated depth, m,
H_{up} – total upstream head above the bottom of the stilling basin, m,
Q – discharge magnitude, m³/s,
b – the width of the stilling basin, m,
φ – velocity coefficient.

$$h_2 = 0.5h_1\sqrt{1+8\frac{\left(\frac{Q}{b}\right)^2}{gh_1^3}} - 1 \tag{2}$$

where:

h_2 – second conjugated depth, m,

$$\Delta H = H_1 - H_2 = \frac{\left(h_1 - h_2\right)^3}{4 \cdot h_1 \cdot h_2} \tag{3}$$

where:

H_1 – total energy head at the cross section of h_1, m,
H_2 – total energy head at the cross section of h_2, m,
ΔH – total energy head loss within the hydraulic jump, m.

Table 1. The calculated depths (d) of the theoretical stilling basin of different widths (5 m and 10 m) and hydraulic jump parameters: conjugated depths – h_1, h_2, energy head loss – ΔH and relative energy head loss – $\Delta H/H_1$ (eq. 3)

q [m²/s]	d [m]	Fr_1 [–]	h_1 [m]	h_2 [m]	ΔH [m]	$\Delta H/H_1$ [%]
5	0	4.8	0.48	3	2.8	47
10	0	3.2	1	4	1.7	29
5	1.2	5.1	0.45	3.2	3.6	52
10	2.5	3.4	0.85	4.5	2.1	40

2.3. Mathematical model of the turbulent flow

The Flow-3D computational fluid dynamics program was used for the numerical solution of the Reynolds-averaged Navier–Stokes (RANS) momentum transport equations (eq. 5) and continuity equations (eq. 4). This program uses the finite volume approach with a staggered grid for discrete representation of the governing equations. All equations are formulated with area and volume porosity functions. This formulation, called the 'fractional area/volume obstacle representation' (FAVOR) method is used to model complex geometric regions and solid boundaries [2]. The volume of fluid (VOF) method is employed in FLOW-3D to properly capture the free-surface of liquid; the additional transport equation is added (eq. 6).

The general governing equations for incompressible flow, including the FAVOR variables, are given by:

$$\nabla \circ \left(\mathbf{u}\mathbf{A}_{\mathbf{f}} \right) = 0 \tag{4}$$

$$\frac{\partial \mathbf{u}}{\partial \mathbf{t}} + \frac{1}{\mathbf{V}_{\mathbf{f}}} \left(\mathbf{u}\mathbf{A}_{\mathbf{f}} \circ \nabla \right) \mathbf{u} = -\frac{1}{\rho} \nabla \mathbf{P} + \mathbf{G} + \mathbf{f} \tag{5}$$

$$\frac{\partial \mathbf{F}}{\partial \mathbf{t}} + \frac{\mathbf{F}}{\mathbf{V}_{\mathbf{f}}} \nabla \circ \left(\mathbf{u}\mathbf{A}_{\mathbf{f}} \right) = 0 \tag{6}$$

where:

- $\mathbf{u}$ – fluid velocity vector, m/s,
- $\mathbf{f}$ – viscous accelerations vector, m/s^2,
- $\mathbf{P}$ – pressure, N/m^2,
- $\mathbf{G}$ – body accelerations vector, m/s^2,
- $\mathbf{V}_{\mathbf{f}}$ – volume fraction, m^3,
- $\mathbf{A}_{\mathbf{f}}$ – area fraction vector, m^2,
- $\mathbf{F}$ – fluid fraction.

The RANS model includes a formulation for the turbulent kinetic energy (k) and the rate of turbulence dissipation (ε) to obtain Reynolds stress (τ_{Rij}) tensor and turbulent viscosity as follows:

$$\tau_{Rij} = \upsilon_t \left[\frac{\partial u_i}{\partial x_j} + \frac{\partial u_j}{\partial x_i} \right] - \frac{2}{3} \delta_{ij} k \tag{7}$$

$$\upsilon_t = 0.9 \frac{k^2}{\varepsilon} \tag{8}$$

where:

- u_i – velocity component $i = 1, 2, 3$, m/s,
- v_t – turbulent viscosity, N · s/m^2,
- k – turbulent kinetic energy, J/kg,
- ε – rate of turbulence dissipation, J/(kg · s),
- τ_{Rij} – Reynolds stress tensor, N/ m^2.

In this work, the k-ε turbulence model was used [1, 2].

2.4. Boundary condition

The upstream face boundary condition is in the form of constant in time flow rate ($Q = 50$ m^3/s) discharged into the chute (Fig. 1) and the downstream face boundary is in the form of constant in time hydrostatic pressure distribution. Tail water head (h_d) at the ending cross section of the channel is equal to 2 m. A constant value of surface roughness coefficient ($k_r = 0.001$ m) was assumed for the solid boundary.

The flux control cross sections (baffle) were defined within the numerical model (Fig. 1) in order to calculate energy loss as result of: the hydraulic jump ($b1$–$b2$); sudden vertical contraction at the ending cross section of the stilling basin ($b2$–$b3$); flow along the short channel reach (6 m length) just downstream of the stilling basin ($b3$–$b4$). Thus, three control volumes were defined. In each baffle, the total hydraulic energy rate is calculated and the flux-averaged total head is then fixed (eq. 8).

$$H_e = \frac{\int_A H \cdot \mathbf{u} \circ \mathbf{n} \cdot dA}{Q} \tag{9}$$

where:

H_e – flux-averaged hydraulic head at control cross section, m,
H – total hydraulic head of streamline at control cross section, m,
$\mathbf{u}$ – resultant velocity vector, m/s,
$\mathbf{n}$ – normal unitary vector,
A – area of control cross section, m^2,
Q – volumetric flow rate, m^3/s.

2.5. Results of the numerical modelling analysis

The results of the numerical modelling for different variants of the stilling basin enabled the evaluation of the hydraulic jump submergence conditions for given values of the design discharge ($Q_d = 50$ m^3/s) and tail water head ($h_d = 2$ m). In the case of S2, the hydraulic jump is fully submerged (Fig. 2), the total head loss magnitude by this hydraulic jump is: $\Delta H_e = 2.65$ m (Table 2) and this value is 0.55 m larger than the calculated value (Table 1) in the case of the hypothetical flow without crosswise expansion ($q = 10$ m^2/s and $d = 2.5$ m). The flow layer under the roller is in the shape of a thin prism (Fig. 2a) – this is consistent with the experimental data relating to velocity distribution characteristics [4]. The velocity magnitude reaches 8.5 m/s in the middle of the stilling basin and decreases at the ending cross section of the stilling basin to a value of 4.5 m/s where the vertical component of the velocity (about 2.1 *m/s*) is dominant.

This large value of the vertical component of the velocity is associated with abrupt flow vertical contraction and a water surface level rise of about 0.25 m above the level of the tail water surface. This surface level increase magnitude is comparable with the magnitude of the energy head loss due to vertical flow contraction (Table 2).

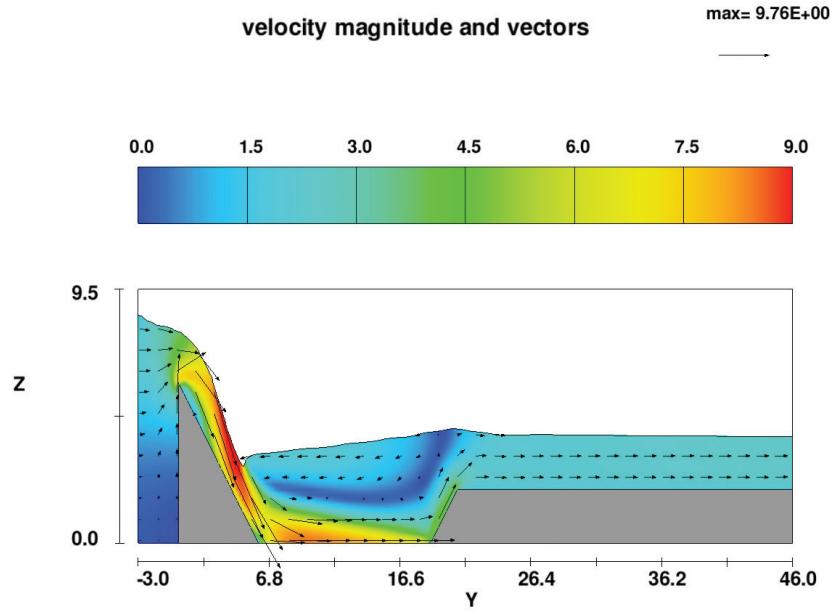

Fig. 2a. Velocity distribution at the central vertical cross section of the stilling basin for the design flow rate condition (case S2)

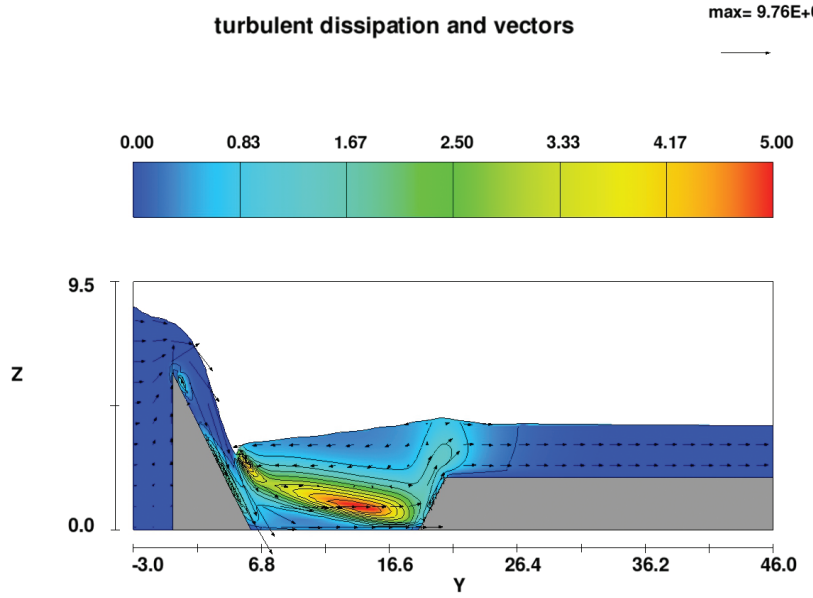

Fig. 2b. Turbulent dissipation rate distribution at central vertical cross section of the stilling basin for the design flow rate condition (case S2)

The turbulent energy dissipation rate magnitude reaches maximum value (5 J/kg/s) within the shear layer about 1 m above the bottom in the middle of the stilling basin (Fig. 2b) and is associated with the maximum magnitude of velocity gradient.

Table 2. Table 2. Flux-averaged hydraulic head (H_e) and head losses (ΔH_e) at flux baffles for different basin cases and for given design discharge (Q_d = 50 m^3/s)

Basin case/ baffle	S2		S1		S05		S05p		S02p	
	H_e [m]	ΔH_e [m]	H_e [m]	ΔH_e [m]	H_e [m]	ΔH_e [m]	H_e [m]	ΔH_e [m]	H_e [m]	ΔH_e [m]
b1	7.57	-	6.56	-	6.15	-	6.15	-	5.96	-
b2	4.92	2.65	4.03	2.53	3.97	2.18	3.35	2.8	3.49	2.47
b3	4.71	0.21	3.54	0.49	3.10	0.87	2.95	0.40	2.99	0.50
b4	4.4	0.31	3.46	0.08	2.95	0.15	2.85	0.10	2.69	0.30

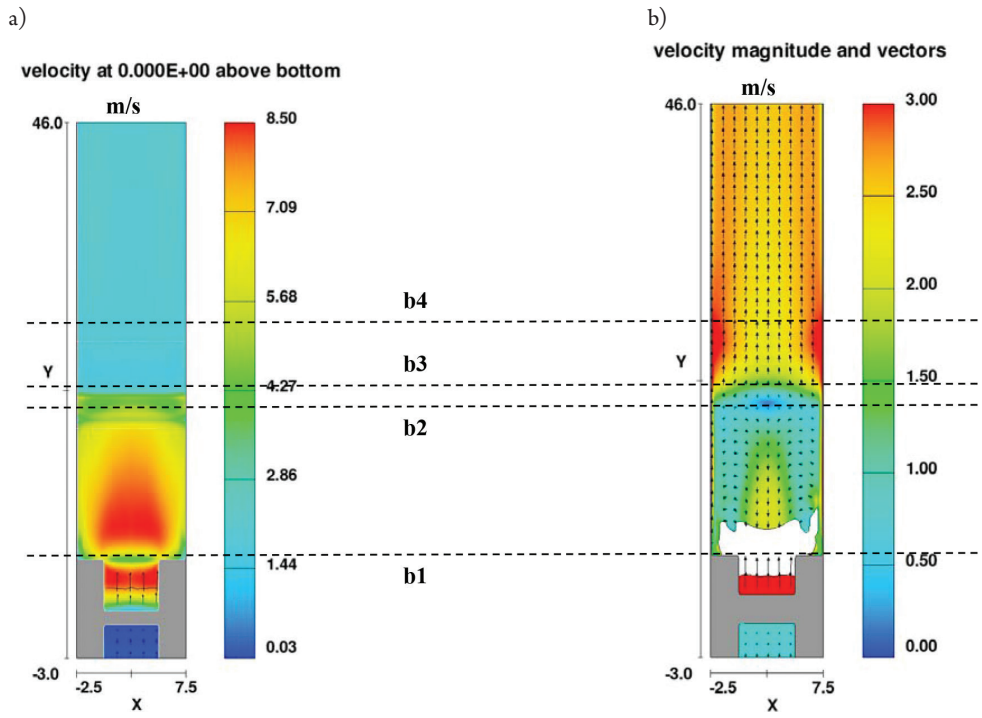

Fig. 3. Velocity distribution: a) at the bottom; b) at a level of 1.5 m above the channel bottom for the design see above note flow rate condition (case S2)

Within the control zone b3–b4 of the channel reach, the value of the turbulent energy dissipation rate is less than 0.5 J/kg/s and velocity is almost uniformly distributed (within the range: 2.8–2.9 m/s) at the downstream cross section of the channel (Fig. 3).

The hydraulic conditions described above are highly acceptable from the point of view of the safe exploitation of the stilling basin *S*2. In spite of this, the hydraulic jump within *S*2 is submerged under the condition of the design discharge and tail water head magnitude, the reduction of depth of the stilling basin will often allow reduced costs of investment; therefore, a stilling basin of lower depths (1 m, 0.5 m and 0.2 m with or without the ending sill) were tested for the determination of the hydraulic condition.

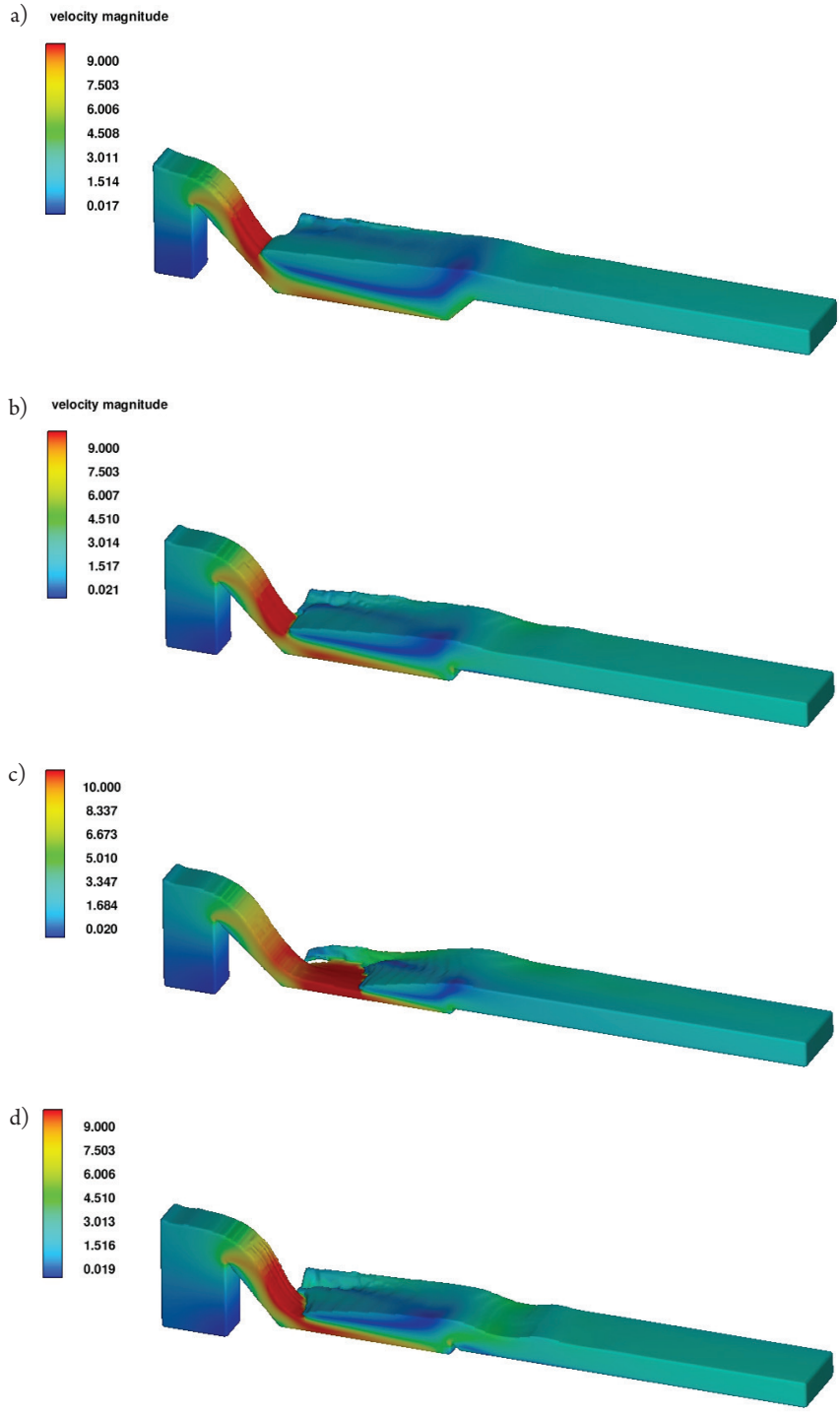

Fig. 4. Spatial velocity distribution (longitudinal symmetrical half of the picture) of the flow domain: a) case S2, b) case S1, c) case S05, d) case S05p

In the case of *S*1, the hydraulic jump is still submerged (Fig. 4b) as is also implied by the simplified calculations for the uniform inflow (q = 5 m^2/s and d = 1.2 m) in a rectangular prismatic channel without crosswise expansion (Table 1). The stream flow expansion within the stilling basin may contribute to the reduction of the sequent conjugated depth of the hydraulic jump, which in the case of *S*1 is equal to 3.2 m based on the results of numerical modelling. In all tested cases, a sudden significant rise in the water surface level close to the sidewalls of the stilling basin is identified (Fig. 4). The significant transversal velocity component magnitude (Fig. 5) contributes to the kinetic energy exchange into the potential energy within sidewall zones.

This energy exchange is the source of additional energy loss and indicates the spatial character of the hydraulic jump.

The significant contribution to kinetic energy dissipation, and thus the sequent conjugated depth of the hydraulic jump reduction, is the effect of the vertical flow contraction due to the vertical ending wall of the *S*1, and the total head loss over the control zone b2–b3 is ΔH_e = 0.5 m (Table 2).

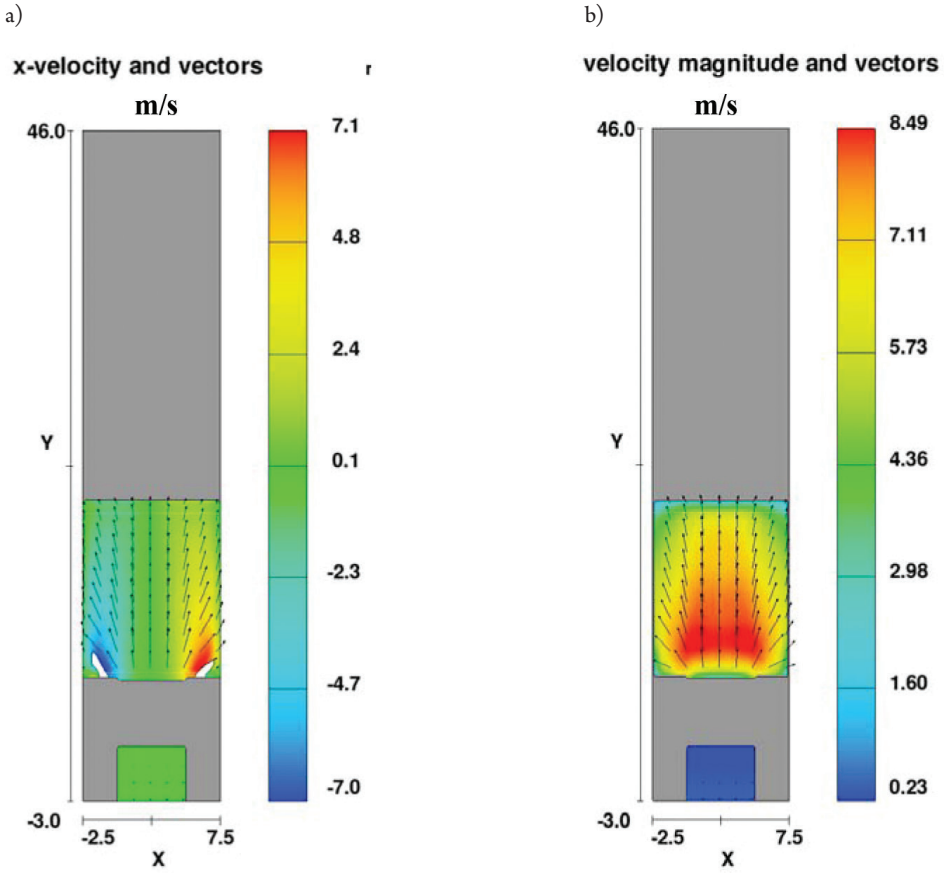

Fig. 5. Velocity distribution at the bottom of the stilling basin: a) x-velocity component; b) resultant velocity magnitude (case *S*1)

As a result of the depth of the stilling basin reducing to 0.5 m, the hydraulic jump is not yet submerged but remains stabilised within the stilling basin (Fig. 4c). In this case, kinetic energy dissipation by the hydraulic jump is ΔH_e = 2.2 m and is smaller than those modelled for other cases, but in the zone of the vertical flow contraction (section b2-b3), the total head loss (ΔH_e = 0.87 m) is the largest in magnitude (Table 2).

Within the stilling basin where supercritical flow condition occurs (Fr = 3), the largest value of bottom shear stress (τ_b = 350 Pa) is identified. Maximum values of the shear stress occur close to the chute outlet and symmetrically on each side (Fig. 6). The shear stress value at the bottom of the channel is not larger than 20 [Pa] and is comparable with other tested cases.

In spite that the hydraulic jump within S05 is not submerged the major energy dissipation occur inside of the stilling basin (Table 2) and at its exit zone therefore total head loss within control section b3-b4 of the channel is small and equal about 0.15 m. It is likely that the unsubmerged hydraulic jump would move downstream due to a small decrease in the tail water surface level; therefore, the impact of the ending sill (h_s = 0.5 m) application within the stilling basin on hydraulic jump submergence was tested (variant S05*p*). In this case, the magnitude of total head loss within control section b1-b2 increases (ΔH_e = 2.8 m) and the hydraulic jump becomes submerged (Fig. 6d).

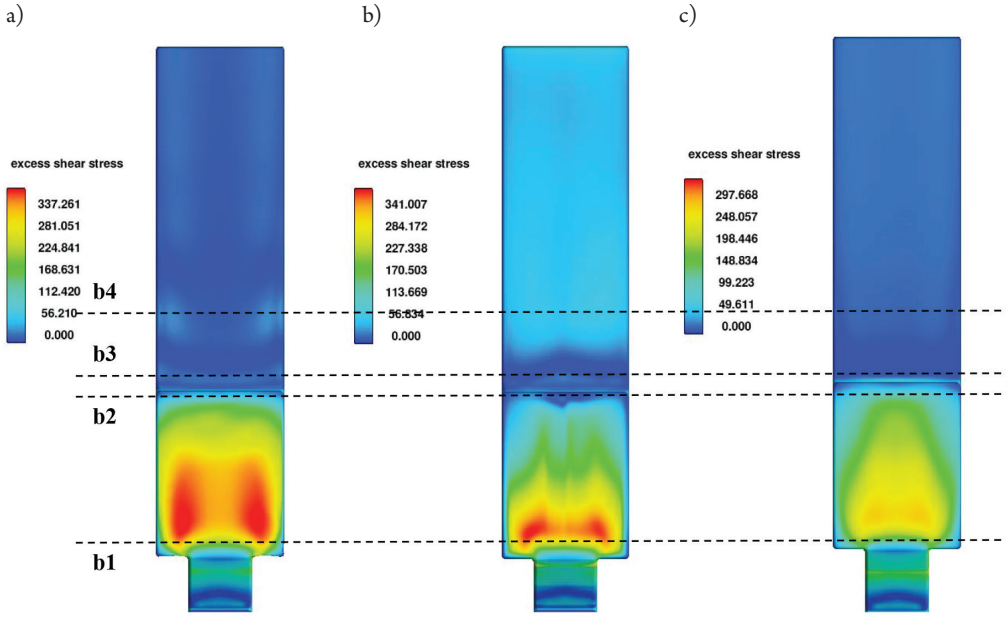

Fig. 6. Shear stress distribution [Pa] at the bottom of the stilling basin and channel: a) case S02*p*; b) case S05*p*; c) case S1

Taking into account cost reduction due to the application of the lower depth stilling basin and fulfilment execution of the hydraulic jump submergence condition, variant S05*p* seems to be optimal. Nevertheless, significant decreasing of the tail water surface level (in this case by 1 m or more) results in the occurrence of unwanted pulsation of the weak supercritical flow (*Fr*<1.6) which could be avoided through the application of solution S1 or S2.

If the depth of the basin was decreased to a value of d = 0.2 and the ending sill was used (variant *S02p*), the hydraulic jump would be not submerged and strong waves on the water table within the channel would be observed (Fig. 7). In this case, a small decrease in the tail water table level may cause motion in the hydraulic jump downstream in the channel leading to potential erosion downstream in the channel. Just downstream of the stilling basin, there are regions with a large magnitude of shear stress gradient (Fig. 6a) which may contribute to the erosion of the channel bottom in regions close to the sidewalls of the channel.

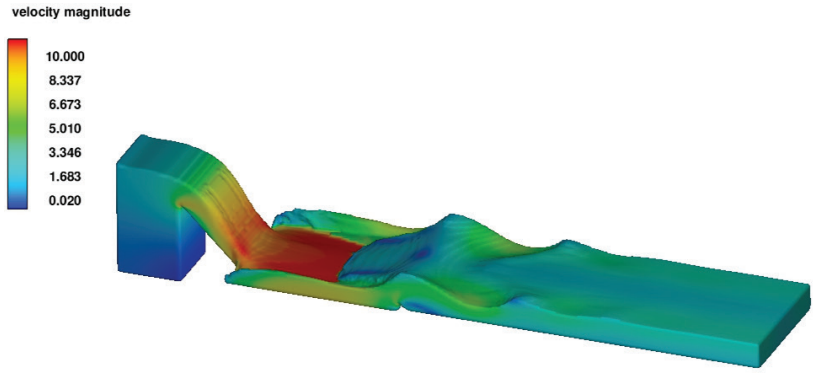

Fig. 7. Spatial velocity distribution and hydraulic jump (case *S02p*)

3. Conclusion

The three-dimensional numerical CFD modelling of the turbulent flow in the stilling basin with sudden crosswise expansion allows the capture of the spatial characteristics of the hydraulic jump and enables testing the influence of the stilling basin depth magnitude changes on the submergence condition of the hydraulic jump. The results of the numerical modelling indicate that such factors as crosswise flow expansion, vertical flow contraction resulting from a stilling basin deepening, and installation of the terminal sill lead to decreases in the sequent conjugated height of the hydraulic jump and to local increases in the level of the tail water table which significantly contribute to the hydraulic jump submergence condition. In the practice it means that the stilling basin of smaller depth than one implies from the one dimensional simplified analysis (in this studied case, depth reduction occurs from 2 m to 1 m or to 0.5 m under condition of the ending sill installation) could be applied to disperse turbulent kinetic energy of the flow from the spillway efficiently. The CFD numerical modelling may contribute to the more realistic designing of the stilling basin and thus may improve the operational safety profile and reduce costs of an investment.

References

[1] Flow Science, Inc., 2014, *FLOW-3D User Manual, Release* 11.0.3, USA 2014.

[2] Matin M.A., Hasan M, Islam M.R., *Experiment on hydraulic jump in sudden expansion in a sloping rectangular channel*, Journal of Civil Engineering (IEB), 36(2)/2008, 65–77.

[3] Urbański J., Siwicki P., *Zastosowanie programu CFD fluent do obliczeń charakterystyk turbulencji strumienia w dolnym stanowisku jazu*, Infrastruktura i Ekologia Terenów Wiejskich, No. 2007/4(2).

[4] Gandhi S., *Characteristics of Hydraulic Jump*, International Journal of Mathematical, Computational, Physical, Electrical and Computer Engineering, Vol. 8, No. 4/2014.

[5] Tannehill J.C., Anderson D.A., Pletcher R.H., *Computational Fluid Mechanics and Heat Transfer*, 2nd Ed., Taylor & Francis, USA 1997.

[6] Bayon-Barrachina A., Amparo Lopez-Jimenez P., *Numerical analysis of hydraulic jumps using OpenFOAM*, Journal of Hydroinformatics, 17(4)/2015, 662–678.

[7] Carvalho R.F., Lemos C.M., Ramos C.M., *Numerical computation of the flow in hydraulic jump stilling basin*, Journal of Hydraulic Research 46(6)/2008, 739–752.

[8] Chanson H., Gualtieri C., *Similitude and scale effects of air entrainment in hydraulic jump*, Journal of Hydraulic Research 46(1)/2008, 35–44.

[9] Mortensen J.D., Barfuss S.L., Johnson M.C., *Scale effects of air entrainment by hydraulic jumps within closed conduits*, Journal of Hydraulic Research, Vol. 49/2011, 90–95.

[10] Ead S. A., Rajaratnam N., *Hydraulic jumps on corrugated beds*, Journal of Hydraulic Engineering, ASCE, Vol. 128, No. 7/2002, 656–663.

[11] Abbaspour A., Farsadizadeh D., Dalir A H., Sadraddini A.A., *Numerical study of hydraulic jumps on corrugated beds using turbulence models*, Turk. J. Eng. Environ. Sci., 33(1)/2009, 61–72.

[12] Amorim Jose Carlos C., Rodrigues Cavalcanti R., Marques Marcelo G.A., *Numerical and Experimental Study of Hydraulic Jump Stilling Basin*, Advances in Hydro-Science and Engineering, Vol. VI/2007.

[13] Peterka A.J., *Hydraulic design of stilling basins and energy dissipators*, Engineering Monograph 25, U.S. Bureau of Reclamation 1963.

[14] Valero D., Bung D., Crookston B., Matos J., *Numerical investigation of USBR type III stilling basin performance downstream of smooth and stepped spillways*, [in:] B. Crookston & B. Tullis (eds.), *Hydraulic Structures and Water System Management*, 6th IAHR International Symposium on Hydraulic Structures, Portland, June 2016, 652–663.

[15] Babaali H., Shamsai A., Vosoughifar H., *Computational modeling of the hydraulic jump in the stilling basin with convergence walls using CFD codes*, Arabian Journal for Science and Engineering., 40(2)/2015, 381–395.

[16] Ven Te Chow, *Open-Channel Hydraulics*, McGraw-Hill, New York 1959.